Available online at www.sciencedirect.com
ScienceDirect
Journal of the European Ceramic Society 29 (2009) 2289–2296
www.elsevier.com/locate/jeurceramsoc

Birefringence measurements of creep near an electrode tip in transparent PLZT

Q.D. Liu [a], N.A. Fleck [a,*], J.E. Huber [b], D.P. Chu [a]

[a] *Department of Engineering, University of Cambridge, Trumpington Street, Cambridge CB2 1PZ, UK*
[b] *Department of Engineering Science, University of Oxford, Parks Road, Oxford OX1 3PJ, UK*

Received 7 November 2008; received in revised form 18 December 2008; accepted 8 January 2009
Available online 13 February 2009

Abstract

Birefringence measurements of time-dependent, creep polarization and strain were made in bulk ceramic samples of PLZT 8/65/35. Two specimen configurations were used: a fixed uniform electric field to measure the creep response and correlate birefringence with strain and polarization, and specimens with a partial surface electrode, to study the local behaviour near the tip of a surface electrode. At low values of electric displacement, the electric displacement depended upon the principal strain difference in a quadratic fashion whereas the birefringence varied linearly with the principal strain difference. Three distinct regimes of switching were identified, corresponding to the nucleation of ferroelectric domains, rapid switching and saturation in the process of domain growth. Finally it is shown that the birefringence measurements near an electrode tip give the spatial evolution of principal strain difference.

Keywords: Ferroelectric; Creep; Birefringence

1. Introduction

When a constant stress or electric field is applied to a ferroelectric, the resulting strain and electric displacement change with time in a creep-like manner. This effect is often neglected in applications where loads are well below the coercive level or where high frequency cyclic loads are used. However, in some technologically important cases, creep or relaxation processes are of practical significance. For example, ferroelectric memory elements are required to maintain a polarization state for long periods of time in a state of residual stress.[1,2] Similarly, the interdigitated electrode tips in stack actuators produce intense local fields that degrade the device performance over time.[3]

Time-dependent behaviour has been reported for various compositions of ferroelectric ceramic.[4,5] Under a uniform, constant electric field or stress loading, the changes in strain and electric displacement can be observed by strain gauges and by surface charge measurements. However, these measurements do not give insight into the spatial variation of non-uniform evolving fields, such as those near an electrode tip. Although several theoretical and experimental studies of the electrode tip problem can be found in the literature,[6–8] the experimental studies rarely give the spatial variation of fields close to the electrode tip, and there is practically no work on the evolution of non-uniform fields with time. Recently, Qiu et al.[9] used Moiré interferometry to observe the static displacement field in the vicinity of an electrode tip. In the present work, the spatial and temporal variation of strain fields is observed in specimens of transparent PLZT 8/65/35 using a standard birefringence system (Metripol microscope, Oxford instruments). In an initial calibration, the birefringence, strain and electric displacement are all measured under a uniform field; these tests indicate that the birefringence can be related to both the principal strain difference and to electric displacement, provided that the value of electric displacement is well below the saturation value. This calibration information is then used to infer the strain and electric displacement state in the vicinity of an electrode tip using birefringence measurements.

2. Birefringence measurement

Anisotropic crystals such as ferroelectrics have distinct refractive indices (n) for waves polarized in different principal

* Corresponding author.
E-mail address: naf1@eng.cam.ac.uk (N.A. Fleck).

0955-2219/$ – see front matter © 2009 Elsevier Ltd. All rights reserved.
doi:10.1016/j.jeurceramsoc.2009.01.008

planes. Light waves propagate in the x_2 direction with refractive index n_1 if polarized in the 1–2 plane and n_3 if polarized in the 3–2 plane. The magnitude of the difference $\Delta n = |n_1 - n_3|$ is the birefringence. Since the wave speed depends on the electron density, Δn is closely related to the principal strain difference, $\varepsilon_{11} - \varepsilon_{33}$, and this is the basis of photoelastic strain measurement.[10] The difference in speed of waves polarized in the 1–2 and 3–2 planes produces a relative phase difference $\delta = 2\pi t \Delta n/\lambda$ when light of wavelength λ passes through a specimen of thickness t. Various systems exist for measuring the phase difference δ and the optical orientation angle φ, corresponding to the orientation of the fast optical axis. In this work, the Metripol microscope (Oxford Cryosystems Ltd.) is used to measure δ over the region of interest of the PLZT specimens. The system has an optical path consisting of a rotating polarizer, the specimen under consideration, a quarter wave plate and an analyser. With the polarizer at angular position α, the transmitted light intensity I is related to δ and φ according to[11]:

$$I = \frac{I_0}{2}\{1 + \sin\delta \sin 2(\varphi - \alpha)\} \quad (1)$$

where $I_0/2$ is the mean transmitted light intensity. By rotating the polarizer through a full cycle $0 \le \alpha \le 2\pi$, and recording birefringence images at several angles, the Metripol system identifies $|\sin\delta|$, φ and $I_0/2$ at each point in the field of view. Measurements made by this technique are discussed further in Sections 4 and 5 of the paper. However, in some of our tests, the transmitted light intensity was too low for the birefringence to be identified directly by the Metripol system. This happens because the poling process in PLZT 8/65/35 converts the material from a transparent state to a scattering (opaque) state. In these cases, no measurement of $|\sin\delta|$ and φ could be made, but it was still possible to obtain measurements of average transmittance by making direct use of the signal from the CCD camera used to collect images in the Metripol system. This technique is used in Section 3 to correlate the optical transmittance with the polarization state.

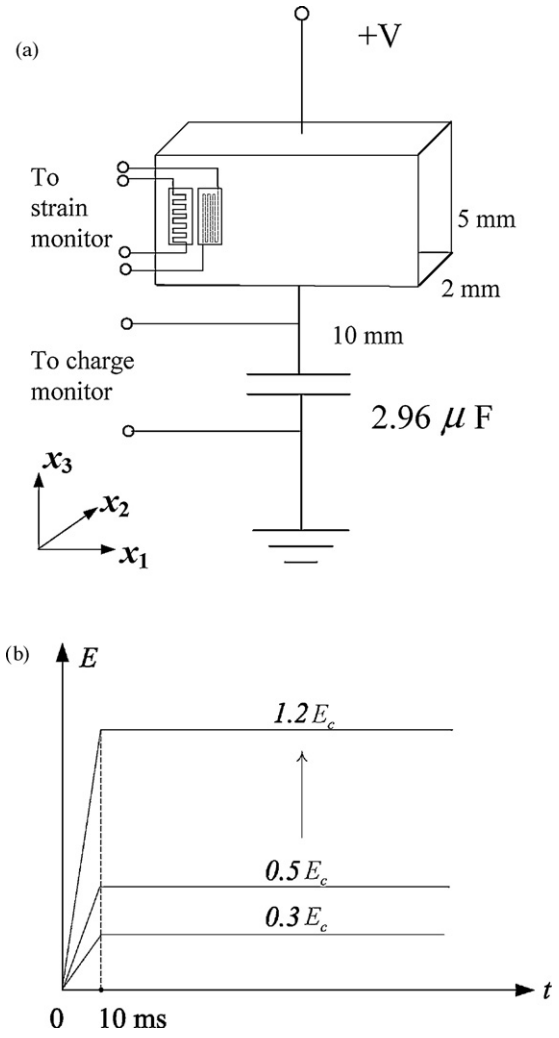

Fig. 1. (a) Specimen arrangement for creep measurements under uniform electric field, showing a PLZT 8/65/35 specimen with the full size electrodes and strain gauges for the measurement of ε_{33} and ε_{11}. (b) The electrical loading profile used for creep measurement. The level of applied electric field varies from $0.3E_c$ to $1.2E_c$.

3. Creep observation in uniform electric field conditions

Bulk PLZT 8/65/35 ceramic with grain size about 1 μm was obtained in the as-sintered state from Alpha Ceramics Inc. The material is optically transparent in the unpoled state, with a low frequency (0.1 Hz) coercive field E_c of 0.4 MV m^{-1} and a saturation polarization $D_0 = 0.32$ C m^{-2}, measured after poling with field strength of $3E_c$ at room temperature. On the PLZT phase diagram, the 8/65/35 composition lies close to the boundaries of cubic (non-polar), tetragonal, rhombohedral and orthorhombic phases[12] and this composition shows relaxor behaviour. Specimens of dimension 2 mm × 5 mm × 10 mm were prepared by dicing from the bulk, and the 5 mm × 10 mm side faces were polished to a 1 μm finish using diamond paste. Each specimen was annealed at 300 °C for 2 h to relieve the residual stresses due to material processing. Electrodes were made using silver-impregnated epoxy, on the 2 mm × 10 mm top and bottom faces. A high-voltage source driven by computer control was connected to one electrode, while the other electrode was grounded through a charge metering capacitor. Strain gauges were adhered to the specimen to measure strains ε_{11} and ε_{33}, perpendicular to the direction of light propagation (see Fig. 1a). Each specimen was immersed in oil in a glass dish, maintained at 18–20 °C, and placed in the optical path of the Metripol system. Checks were made to confirm that the apparatus was optically isotropic when the PLZT specimen was absent. It should be noted that, under strong electric field conditions, it is possible for a circulation of the insulating oil to arise, causing some optical anisotropy. However, this effect was not observed at the field strengths used in the present work. A voltage signal consisting of a rapid rise in voltage over about 10 ms, followed by constant voltage held for several minutes, was applied to each unpoled specimen, see Fig. 1b. The time evolution of strain components ε_{33} and ε_{11} and of the electric displacement component D_3 was recorded. Simultaneously, birefringence measurements were made by focusing the birefringence microscope on a region of material about 2.8 mm × 1.8 mm in area near the specimen centre; in each case, a nearly uniform optical response was detected.

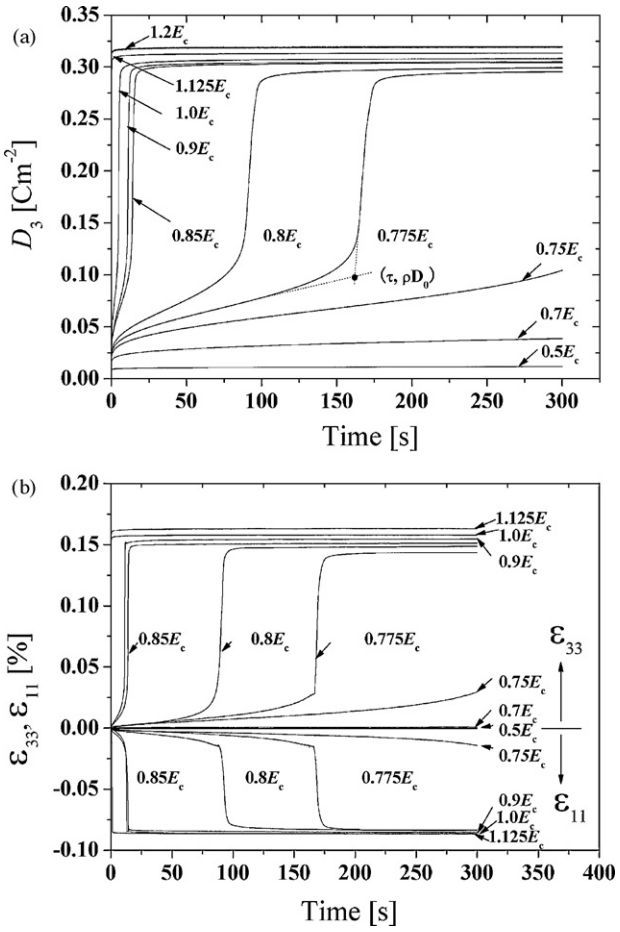

Fig. 2. (a) Measured electric displacement (D_3) values versus time at different levels of applied electric field E. Characteristic parameters τ and ρD_0 are shown for the case $E = 0.775E_c$. (b) Measured ε_{33} and ε_{11} values versus time at different levels of electric field E.

The measured $D_3(t)$, $\varepsilon_{33}(t)$, and $\varepsilon_{11}(t)$ responses over the first 300 s of electrical loading are shown in Fig. 2. The $D_3(t)$ response suggests that the switching process can be divided into three stages: an initial stage of gradual polarization increase up to about 0.08 C m^{-2}, a rapid switching stage over which $D_3(t)$ increases from about 0.08 C m^{-2} to about 0.3 C m^{-2}, and finally saturation of the switching process. This form of time dependence is suggestive of a nucleation, growth and saturation process as described by Johnson–Mehl–Avrami–Kolmogorov models, widely used for interpreting rate effects in ferroelectric films.[13,14] In PLZT 8/65/35, the first stage, where $D_3 < 0.08$ C m^{-2}, is thought to correspond to the build up of macrodomains from an initial disordered state.

A critical value of the polarization, $D_c \approx 0.08$ C m^{-2}, can be identified at the onset of rapid switching. The value D_c is defined in Fig. 2a by the point of intersection of the tangents to the two linear regions of D_3 versus time at around 0.05 C m^{-2} and 0.15 C m^{-2}, respectively. This point also defines a time τ at which the onset of rapid switching begins in each specimen. It is clear from Fig. 2a that the observed threshold value of $D_c \approx \rho D_0$ is independent of the applied electric field. Interestingly, the $\rho = 0.25$ value is close to the percolation probability for site percolation on the FCC lattice.[15]

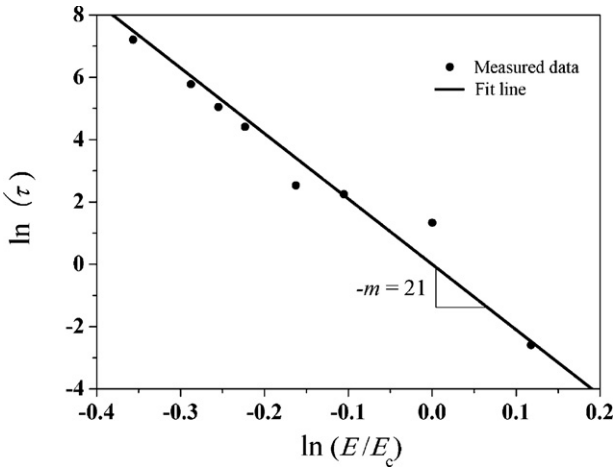

Fig. 3. Time at the onset of rapid switching, τ, versus E/E_c, on logarithmic scales; a straight line fit gives $m = 21$ as the power law creep exponent.

When $E < 0.775E_c$, the polarization responses in Fig. 2 do not reach D_c within the 300 s period of the test. Additional tests of extended duration up to 20 h were performed and the resulting values of ln(τ) (with τ given in units of s) are shown versus ln(E/E_c) in Fig. 3: a power law relation is evident between τ and E. It was also noted that in the early stages of switching ($D < D_c$), the remnant polarization rate $\dot{P}_3^r$ is constant. Consequently, the power law creep relation proposed in previous work for $D < D_c$[5] is satisfied

$$\dot{P}_3^r = \dot{P}_0(E_3/E_c)^m \tag{2}$$

where $\dot{P}_0$ is a reference rate and m is the creep power law exponent for the material. At time τ, this relation implies $D_c = \dot{P}_0(E_3/E_c)^m\tau$ and a power law relation between τ and E results. The straight line fit in Fig. 3 corresponds to power law exponent $m = 21$ and $\dot{P}_0 = 0.1$ C m^{-2}s^{-1}. This high value of power law exponent closely matches previous findings in soft PZT.[5] Belov and Kreher[6] give further support to a power law rate equation and argue that it is a special case of the Arrhenius equation when the applied field is close to the coercive value.

The time evolution of principal strain difference ($\varepsilon_{33} - \varepsilon_{11}$) is given in Fig. 2b for selected values of E. The response is qualitatively similar to that shown in Fig. 2a for the electric displacement D. A cross-plot of ($\varepsilon_{33} - \varepsilon_{11}$) versus D_3 is given in Fig. 4: each line shows the time-dependent growth in $\varepsilon_{33} - \varepsilon_{11}$ and D_3 for fixed values of E. The data suggest a unique quadratic relationship between strain and polarization when $D_3 \le D_c$. This relationship for $D_3 \le D_c$ is confirmed in Fig. 5 by replotting the data in the form of $(D_3/D_0)^2$ versus $\varepsilon_{33} - \varepsilon_{11}$. At greater values of D_3 the electric displacement versus strain relationship is dependent upon the applied field strength, and no unique curve is obtained. The final stages of switching show an increase in electric displacement with little or no strain change, suggesting that 180° switching processes dominate this final stage.

Fig. 6 shows a selection of the time-dependent electric displacement responses normalized by the final (maximum) value of electric displacement D_{max} achieved in each test. Since the optical transmittance of these specimens was rather low, we

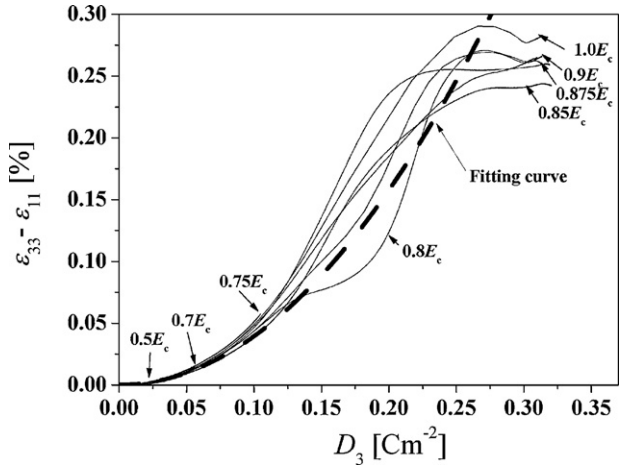

Fig. 4. Measured principal strain difference ($\varepsilon_{33} - \varepsilon_{11}$) versus electric displacement D_3 when different levels of constant electric field are applied.

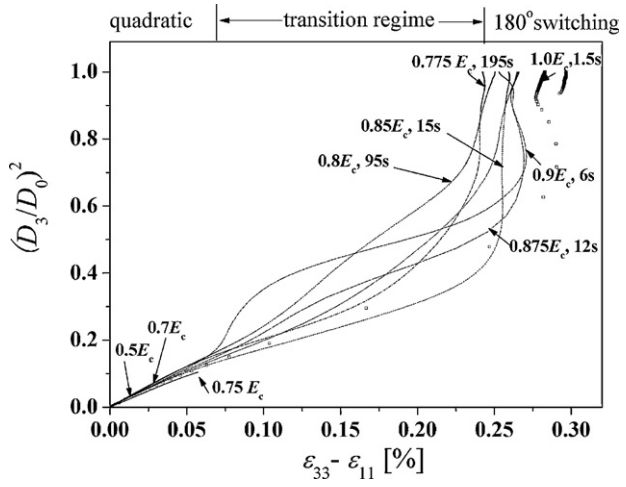

Fig. 5. Normalized electric displacement $(D_3/D_0)^2$ versus ($\varepsilon_{33} - \varepsilon_{11}$) when different levels of constant electric field are applied.

found that the Metripol system was unable to identify $|\sin\delta|$, φ and $I_0/2$ directly throughout the tests. However, by averaging the CCD camera response over a nearly uniform region of 50×50 pixels recorded from close to the centre of the camera

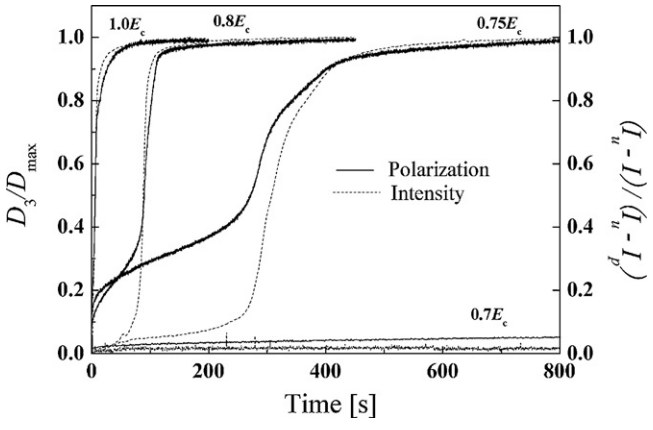

Fig. 6. Normalized light intensity and normalized electric displacement (D_3/D_{max}) versus time for constant electric fields $E = 0.75E_c$, $0.8E_c$ and $1.0E_c$.

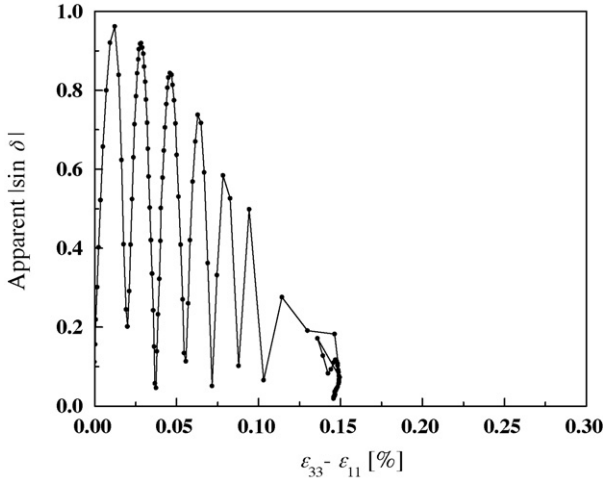

Fig. 7. Measured $|\sin\delta|$ versus principal strain difference ($\varepsilon_{33} - \varepsilon_{11}$) under applied electric field loading $E = 0.725E_c$.

image, it was possible to sample the transmitted light intensity I at 25 Hz sampling frequency, throughout the test. The transmitted intensity varied from an initial value I_U in the unpoled state to a final value I_P in the poled state. The evolution of $(I_U - I)/(I_U - I_P)$ with time is shown in Fig. 6. A strong correlation is seen between the optical transmissivity and the polarization state of the PLZT 8/65/35, as expected.[16,17]

4. Strain – birefringence correlation

Specimens of reduced thickness were used to increase the optical transmittance and thus enable the Metripol system to calculate $|\sin\delta|$, φ and $I_0/2$ values. The specimens were prepared as in Section 3, but polished down to a thickness of 0.36 mm. As before, specimens were placed in the optical path of the Metripol system, and the microscope was focused on the centre of the specimen. The time needed to rotate the polarizer and to compute the resulting birefringence images were such that the optical measurements were made over successive time intervals of 8 s.

Fig. 7 shows a typical $|\sin\delta|$ versus ($\varepsilon_{33} - \varepsilon_{11}$) response taken during a test at constant electric field $E = 0.725E_c$. The values of $|\sin\delta|$ cycle several times during this test, indicating that multiple orders of birefringence are reached ($\delta \gg \pi$). The peak value of $|\sin\delta|$ reached in any given order is expected to be close to 1.0, corresponding to $\delta = (2n-1)\pi/2$ in the nth order. A value close to 1.0 is reached during the first order, but subsequent peaks appear reduced in amplitude. This apparent reduction in amplitude is related to the loss of transparency in the specimens. As optical transmittance is lost, the light intensity shifts away from the linear region of camera response, and the CCD output becomes saturated. This results in a reduced value of the apparent $|\sin\delta|$. This difficulty, which is a consequence of the transparent – scattering transition in PLZT, means that the $|\sin\delta|$ values are not reliable here. However, it is still possible in Fig. 7 to see the sharp reversals corresponding to points where $\sin\delta = 0$. We expect these points to be reliable as they correspond to points of minimum amplitude in the variation of light intensity seen during

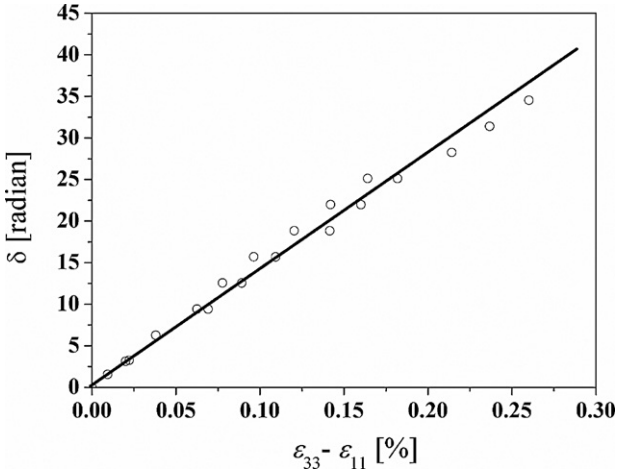

Fig. 8. Birefringence phase difference δ versus principal strain difference $\varepsilon_{33} - \varepsilon_{11}$.

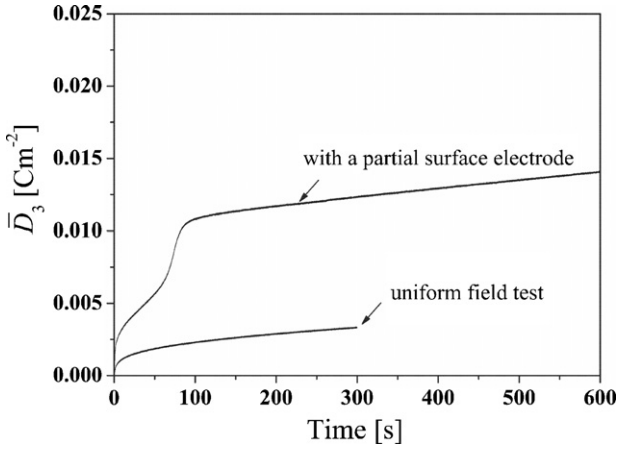

Fig. 10. Measured average surface charge density on the bottom electrode ($\bar{D}_3$) versus time under nominal electric field $E = 0.5E_c$.

a full cycle of the polarizer. The positions of these minima are unaffected by the linearity of the camera response. Taking each successive sharp reversal in Fig. 7 to correspond to an increase in the value of δ by π, it is possible to construct a plot of δ versus $\varepsilon_{33} - \varepsilon_{11}$ as shown in Fig. 8. Here, data points corresponding to the sharp reversals in Fig. 7 are shown, along with additional data taken in the same way from tests with various values of applied electric field. A linear relationship between phase shift δ and principal strain difference $\varepsilon_{33} - \varepsilon_{11}$ is seen over a wide range of strain states.

5. Evolution of birefringence near an electrode tip

Specimens of thickness 0.36 mm with 5 mm × 10 mm polished surfaces were prepared with a partial upper electrode, as shown in Fig. 9. The upper electrode was produced by masking half of one 0.36 mm × 10 mm surface, then applying electrode paint, and finally removing the mask to produce a sharp electrode edge. The length of the upper electrode is about half that of the full lower electrode, and the Metripol microscope was focused on a small region of interest measuring 1.8 mm × 2.8 mm near the edge of the upper electrode. A step voltage was applied at the upper electrode, as in the previous creep measurements. In this case, a 1000 V step was used, corresponding to a nominal electric field strength of $0.5E_c$ between the electrodes. Because of the partial upper electrode, a non-uniform electric field is expected in the region close to the electrode tip.

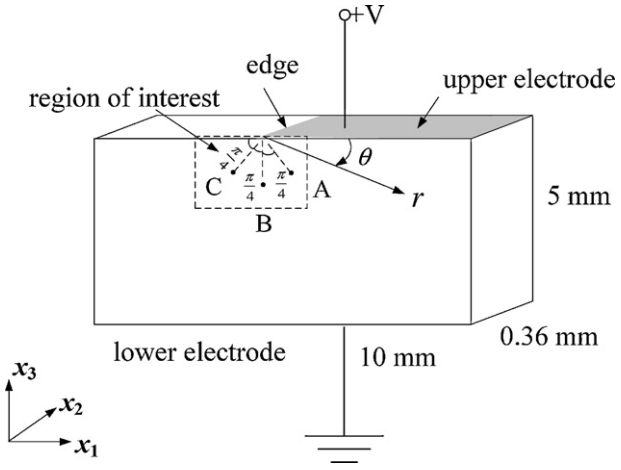

Fig. 9. Specimen arrangement for measuring creep near an electrode tip, showing a PLZT 8/65/35 specimen with a partial upper electrode. Three positions at $r = 1$ mm and $\theta = \pi/4$, $\pi/2$, and $3\pi/4$ are labelled as A, B and C, respectively.

The average charge density $\bar{D}_3$ on the lower electrode versus time is given in Fig. 10 for a specimen with a partial electrode on the upper surface and for a specimen with a full upper electrode (uniform field), respectively. In both cases a nominal electric field strength of $0.5E_c$ was applied between the electrodes. In the case of a partial upper electrode, there is an accelerated switching process due to the non-uniform field conditions introduced by the partial electrode, and this effect dominates the switching behaviour.

Fig. 11 shows birefringence images of $|\sin\delta|$ and φ taken from the region of interest after various time intervals up to 600 s after the voltage was applied. Each image shows data collected during an 8 s period in which the polarizer was rotated. Images are shown in a vertical series corresponding to the state just before the voltage was applied (0 s) and then 8 s, 32 s, 120 s, and 600 s after application of the voltage. Although care was taken to eliminate polishing scratches and to relieve residual stresses, some inhomgeneity due to specimen processing can still be seen in the initial images at 0 s in Fig. 11. The Metripol microscope is very sensitive to strain state, and consequently slight deviations from the isotropic state are detected. The birefringence images evolve with time as fringes radiate away from the electrode tip. The fringes were found to remain after unloading to zero voltage, indicating a remnant strain state.

It is possible to associate a value of principal strain difference with each point in the $|\sin\delta|$ image once the outermost fringe of the radiating pattern has been attributed to the first order of birefringence, with successive fringes representing higher orders. Note, however, the orientation of the principal axes is no longer aligned with the global x_1 and x_3 axes, but varies throughout the region of interest. The time evolution of local principal strain difference is given in Fig. 12 for the three points A, B and C as

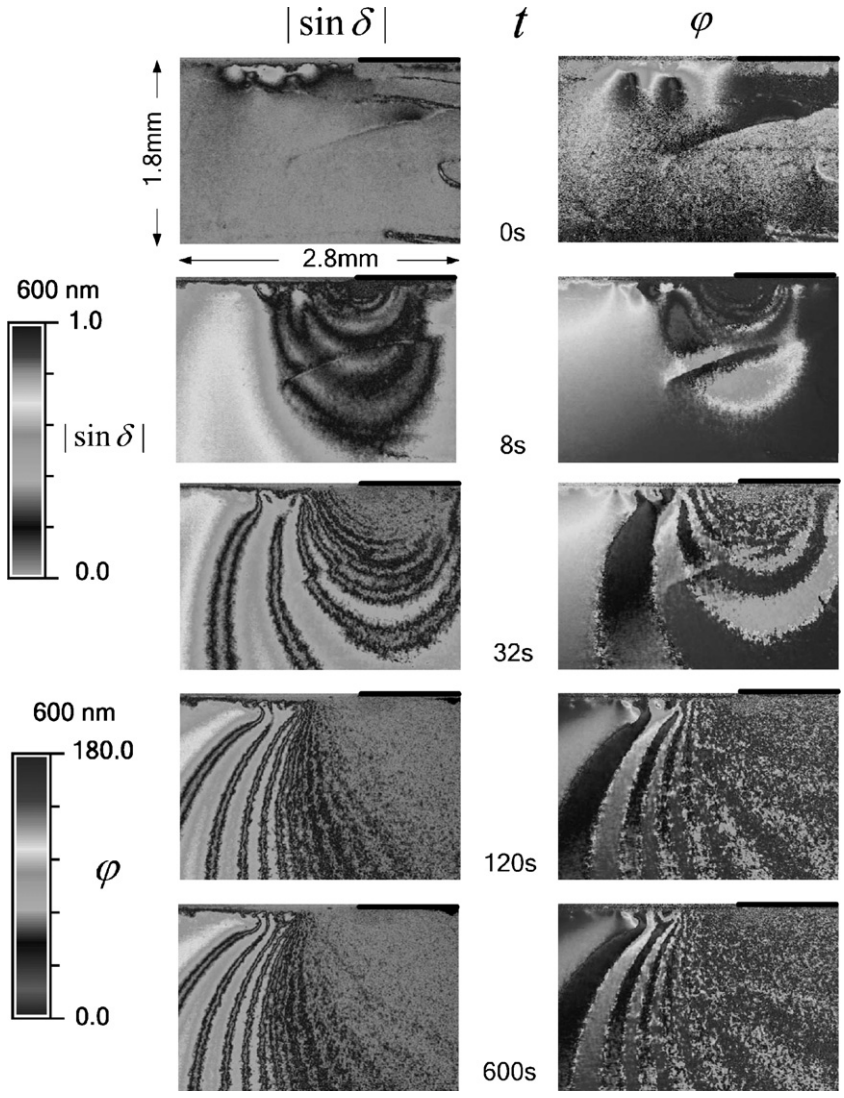

Fig. 11. Birefringence measurements showing the evolution of $|\sin\delta|$ and φ near the electrode tip under an applied electric field $E = 0.5E_c$. The upper electrode is marked by a black line. Note that $\varphi = 0$ is in the direction of x_1.

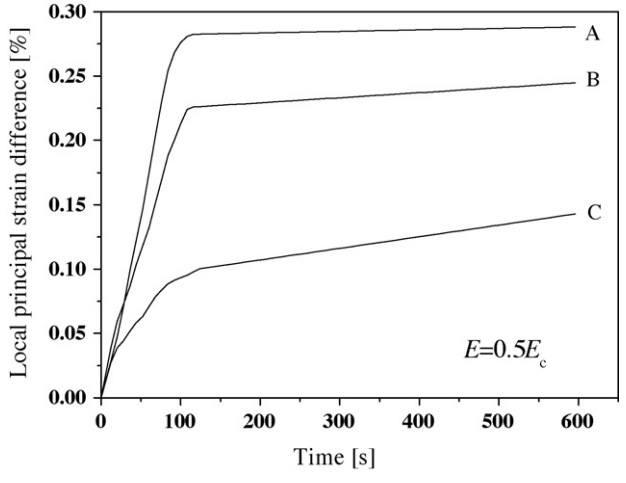

Fig. 12. Time dependence of the local principal strain difference at the positions, A, B and C.

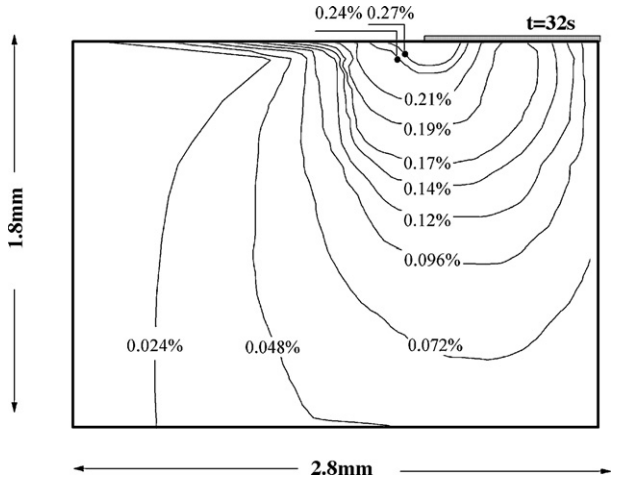

Fig. 13. Contours of principal strain difference near the upper electrode edge, after 32 s.

located in Fig. 9; each point is located 1 mm from the electrode tip but at a different angular location.

Fig. 13 shows a contour plot of the principal strain difference in the region around the electrode tip, corresponding to the birefringence image measured after 32 s application of the electric field. In this material, full switching corresponds to a principal strain difference of approximately 0.25% as indicated in Fig. 2b. Saturated material, with principal strain difference greater than 0.25% exists very close to the electrode tip and will possess a linear response. However, nearly all of the region shown in Fig. 13 has a principal strain difference in the range 0–0.25% and is in the process of switching. The spacing of the strain contours in the region around the electrode tip does not follow the $r^{-1/2}$ singularity that would be expected for linear material behaviour, and is closer to r^{-1}, consistent with non-linear behaviour without significant hardening.

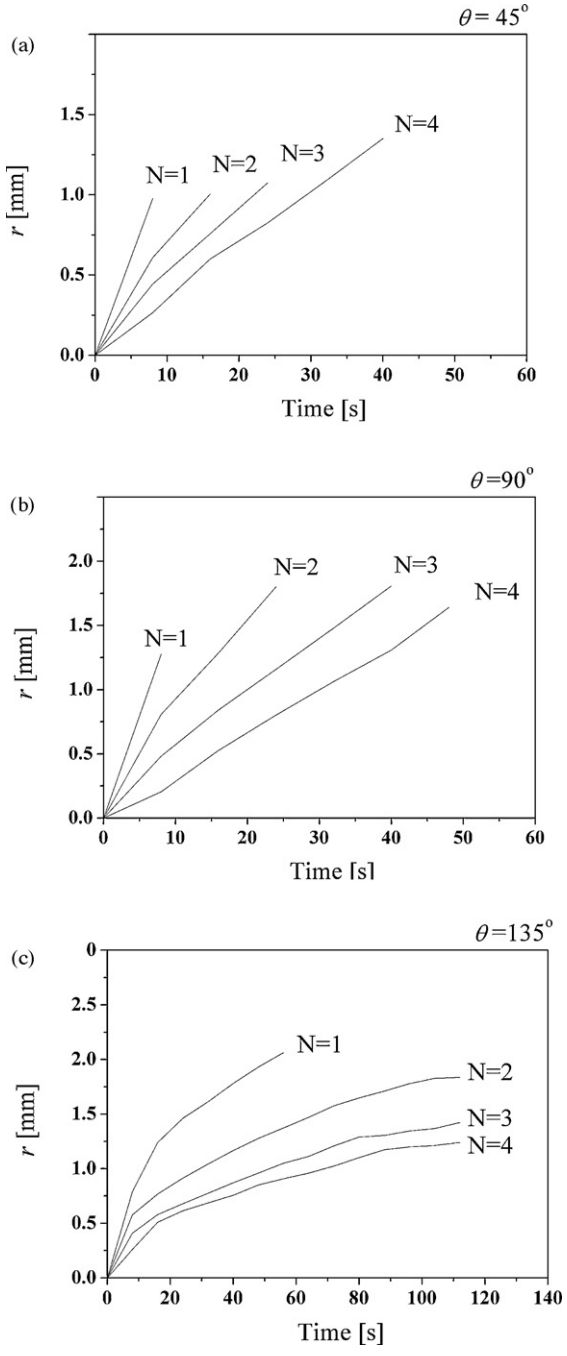

Fig. 14. Radial position r versus time, for the Nth-order fringe, in the directions (a) $\theta = 45°$, (b) $\theta = 90°$ and (c) $\theta = 135°$. The nominal electric field strength was $0.5E_c$. The change in principal strain difference between adjacent orders is 0.024%.

It is of interest to consider the propagating front of the switched region as it radiates away from the electrode tip during this creep test. Using the birefringence measurements, the progress of individual fringes can be tracked. The change in principal strain difference between adjacent fringes is 0.024%, so that the first order fringe corresponds to material at about 10% of the saturation strain, and so forth. Fig. 14 shows the radial distance from the electrode tip reached by the Nth-order fringe as a function of time. The results are shown for each of three angular positions: $\theta = 45°$, 90°, 135°. In Fig. 14c, at $\theta = 135°$, the fringes are seen to be slowing as they move away from the electrode tip into the region of material ahead of the electrode. In this region, the absence of an electrode at the upper surface prevents material from polarizing towards the x_3 direction and the electric field strength reduces towards zero as distance r becomes large. Thus each fringe moves a limited distance from the electrode tip. In contrast, regions with $\theta \leq 90°$ lie between the electrodes and can become fully polarized in the x_3 direction. The first 10 fringes (the tenth corresponding to a fully saturated state) are thus expected to pass through the region between electrodes. This is consistent with the steady progress of the first four fringes seen in Fig. 14a and b.

The transparent PLZT 8/65/35 material differs from ordinary PZT compositions in having relaxor behaviour, which gives the form of creep response recorded in Fig. 2, in contrast to that reported for soft PZT.[5] However, the behaviour becomes quite similar to that of soft PZT once domains have nucleated ($D > D_c$). Using the strain–electric displacement correlation of Fig. 4 suggests that the region near the electrode tip is dominated by material with $D > D_c$. We can thus speculate that the strain contours in an ordinary soft PZT would follow a similar pattern, though the opaqueness of the material would prevent measurement by the birefringence method.

6. Conclusions

Creep in PLZT 8/65/35 due to uniaxial electric field, starting from the unpoled state, shows complex behaviour. Three stages are observed: in the first, the polarization increases to a critical level, corresponding to the growth of macrodomains. This growth correlates with a change from transparent to translucent (scattering) optical behaviour and the rate of growth is a power law function of the electric field. Beyond the critical polarization level, rapid switching and saturation occur. The rapid switching stage is characterised by extensive 90° type, or other strain producing, domain switches.

Time-dependent birefringence was observed near an electrode edge under a constant impressed voltage. The birefringence phase difference correlates well with principal strain difference, allowing the evolution of the strain field distribution

around the electrode edge to be measured. These measurements are useful as a means of validating quantitative ferroelectric switching models.

Acknowledgments

This work forms part of the research programme of the Netherlands Institute for Metals Research (NIMR) and the Stichting voor Fundamenteel Onderzoek der Materie (FOM). The authors are grateful to A.G. Evans for suggestions on the test methods.

References

1. Traynor, S. D., Sun, S. and Hadnagy, D., Capacitor test simulation of retention and imprint characteristics for ferroelectric memory operation. *Integr. Ferroelectr.*, 1997, **16**, 63–76.
2. So, Y. W., Kim, D. J., Noh, T. W., Yoon, J. G. and Song, T. K., Polarization-switching mechanisms for epitaxial ferroelectric Pb(Zr,Ti)O-3 films. *J. Korean Phys. Soc.*, 2005, **46**, 40–43.
3. Janocha, H. and Kuhnen, K., Real-time compensation of hysteresis and creep in piezoelectric actuators. *Sens. Actuators A: Phys.*, 2000, **79**, 83–89.
4. Zhou, D. and Kamlah, M., Determination of room temperature creep of soft lead zirconate titanate piezoceramics under static electric fields. *J. Appl. Phys.*, 2005, **98** [Article 104107].
5. Liu, Q. D. and Huber, J. E., Creep in ferroelectrics due to unipolar electrical loading. *J. Europ. Ceram. Soc.*, 2006, **29**, 2799–2806.
6. Belov, A. Y. and Kreher, W. S., Micromechanics of ferroelectrics: from domain walls to piezoceramic devices. *Ferroelectrics*, 2007, **351**, 79–87.
7. Lucato, S. L. D. E., Lupascu, D. C., Kamlah, M., Rodel, J. and Lynch, C. S., Constraint-induced crack initiation at electrode edges in piezoelectric ceramics. *Acta Mater.*, 2001, **49**, 2751–2759.
8. Prume, K., Gerber, P., Kugeler, C., Roelofs, A., Bottger, U., Waser, R. *et al.*, Simulation and measurements of the piezoelectric properties response (d_{33}) of piezoelectric layered thin film structures influenced by the top electrode size. *Proc. 14th IEEE Int. Symp. Applic. Ferroelect.-ISAF-04*, 2004, **vol. 1**, 7–10.
9. Qiu, W., Kang, Y.-L., Qin, Q.-H, Sun, Q.-S. and Xu, F.-Y., Study for multilayer piezoelectric composite structure as displacement actuator by Moire interferometry and infrared thermography experiments. *Mater. Sci. Eng. A: Struct. Mater. Properties Microstruct. Process.*, 2007, **452**, 228–234.
10. ASTM-D4093-95. *Standard Test Method for Photoelastic Measurements of Birefringence and Residual Strains in Transparent or Translucent Plastic materials*. American Society for Testing and Materials, 2001.
11. Glazer, A. M., Lewis, J. G. and Kaminsky, W., An automatic optical imaging system for birefringent media. *Proc. R. Soc. Lond. A*, 1996, **452**, 2751–2765.
12. Keve, E. T. and Bye, K. L., Phase identification and domain structure in PLZT ceramics. *J. Appl. Phys.*, 1975, **46**, 810–818.
13. Scott, J. F., *Ferroelectric Memories*. Springer, 2000.
14. Ganpule, C. S., Roytburd, A. L., Nagarajan, V., Hill, B. K., Ogale, S. B., Williams, E. D. *et al.*, Polarization relaxation kinetics and 180° domain wall dynamics in ferroelectric thin films. *Phys. Rev. B*, 2001, **65** [Article 014101].
15. Essam, J. W., Percolation theory. *Rep. Prog. Phys.*, 1980, **43**, 833–912.
16. Ivey, M. and Bolie, V. W., Birefringent light scattering in PLZT ceramics. *IEEE Trans. Ultrason. Ferroelectr. Freq. Contr.*, 1991, **38**, 579–584.
17. Land, C. E., Variable birefringence, light scattering and surface-deformation effects in PLZT ceramics. *Ferroelectrics*, 1974, **7**, 45–51.